MOLECULAR STRUCTURE CHANGES OF RABBIT'S RETINA ASSOCIATED WITH HORMONAL CHEMOTHERAPY TREATMENT

HEBA S. GHAZALY[**], *EMAN M. ALY*[*#], *MONA S. TALAAT*[**], *E.M. ELSAYED*[**]

[*] Biophysics and Laser Science Unit, Research Institute of Ophthalmology, Giza, Egypt,
[#]e-mail: e.aly@hotmail.com
[**] Biophysics Branch, Faculty of Science, Ain Shams University, Abbasia, Cairo, Egypt

Abstract. Tamoxifen is an antiestrogen therapy frequently used in the treatment of breast cancer and is currently being assessed as a prophylactic for those at high risk of developing tumors. This study was undertaken to estimate the incidence of retinal changes associated with tamoxifen treatment. Rabbits were divided into four groups, the first group served as control and the other three groups were administered a daily dose of 5, 10 and 15 mg/kg of tamoxifen. Rabbits were decapitated after 2, 4 and 6 months, respectively. Fourier transform infrared (FTIR) spectroscopy and curve-fitting analysis were carried out. Analysis of variance was used with significance level set at $p < 0.05$. The region NH-OH indicates significant changes ($p < 0.05$) in wavenumber and band width. The conformational changes of the secondary structure of the protein in terms of alpha-helixes, beta-sheets and beta-turns were observed in all tamoxifen groups. Also the fingerprint regions indicate changes in the surrounding environment for the administration of tamoxifen. These data indicate a molecular mechanism by which tamoxifen cause retinal secondary structure changes formation suggesting that people using tamoxifen should receive an eye exam at least as often as recommended for middle-aged people.

Key words: Chemotherapy, tamoxifen, rabbit, retina, FTIR.

INTRODUCTION

The increased use of chemotherapeutic agents has resulted in longer cancer patient survival. Consequently, the ophthalmologist is seeing more patients with adverse ocular side effects secondary to these antineoplastic agents [21]. Ocular toxicity induced by cancer chemotherapy includes a broad spectrum of disorders reflecting the unique anatomical, physiological and biochemical features of the eye. Visual changes have been attributed to a number of chemotherapeutic agents such as antimetabolites, alkylating agents, taxanes and hormones [20].

Received: September 2015;
in final form September 2015.

ROMANIAN J. BIOPHYS., Vol. 25, No. 3, P. 185–200, BUCHAREST, 2015

Hormonal therapy is another form of systemic therapy. It is used as an adjuvant/neoadjuvant therapy to help reduce the risk of the recurrent-after surgery/metastasis cancer. Estrogen (ER) is known to promote the growth of about 2 out of 3 of breast cancers (ER-positive cancers) those having receptors for the hormones estrogen and/or progesterone (PR-positive cancers). Because of this, several approaches to blocking the effect of estrogen or lowering estrogen levels are used to treat hormone receptor-positive breast cancers [23].

Tamoxifen is an anti-estrogen drug that selectively modulates the esterogen receptors (SERMs) [3] therefore it can potentially affect the vision as the retina contains estrogen receptors [9].

Decreased visual acuity, bilateral macular edema, retinal yellow-white dots and corneal opacities, bilateral optic neuritis and retinal hemorrhages have been reported [2, 22]. Gorin *et al*. [14] described intra-retinal crystals and posterior sub-capsular opacities with tamoxifen usage. On the whole, the most common tamoxifen induced ocular toxicities remain to be the retinopathy and cataract, lesions of cornea and optic nerve. Salomao [25] concluded that the aspects of central retinal function that are assessed by multifocal ERG were not affected after tamoxifen use, suggesting that the multifocal ERG is not sufficiently sensitive to detect tamoxifen-associated changes that might occur, although there was a degree of color vision loss and ocular toxic effects were found in some cases of this cohort. Chung *et al*. [6] stated that patients with low cumulative doses of tamoxifen can also suffer visual symptom-related foveal cystoid spaces and/or macular thinning. Cho *et al.* [5] investigated the mechanism of tamoxifen retinotoxicity using human retinal pigment epithelial (RPE)-derived (ARPE-19) and photoreceptor-derived (661W) cells and found that lysosomal membrane permeabilization as well as caspase-dependent apoptosis contributed to tamoxifen-induced cell death.

Anticipation of various treatment related toxicities may also provide the opportunity to develop intervention strategies that could minimize expected adverse effects. Therefore this study aims to understand the causation of tamoxifen ocular toxicity in particular its molecular structure retinal changes.

MATERIALS AND METHODS

MATERIALS

Sixty healthy New Zealand white rabbits of either sex, weighing 2–2.5 kg were randomly selected from the animal house facility at the Research Institute of Ophthalmology RIO, Giza, Egypt. The animals were kept separately under good ventilation and adequate standard diet. They were housed in special designed cages and maintained under constant air flow and illumination during the experimental periods, also away from any acoustic stress or electromagnetic radiation. The

animal was handled according to the ARVO (The Association for Research in Vision and Ophthalmology) statements and regulations for the use of animals in research. The rabbits were divided into 4 main groups:

Control group: (n = 15) kept untreated as a normal group.

Tamoxifen administered group: (n = 15) received orally daily dose of 5 mg/kg (D_5).

Tamoxifen administered group: (n = 15) received orally daily dose of 10 mg/kg (D_{10}).

Tamoxifen administered group: (n = 15) received orally daily dose of 15 mg/kg (D_{15}).

Rabbits groups were subdivided into three subgroups and decapitated after 2, 4 and 6 months, respectively (T_2, T_4, and T_6).

ADMINISTRATION OF TAMOXIFEN

Tamoxifen (Nolvadex, AstraZeneca-Egypt) was administered orally through the stomach tube once with doses 5, 10 and 15 mg/kg tamoxifen/day by gastric intubation in 0.5% hydroxypropyl methylcellulose [15] at 5 mL/kg dose volume between 09 and 10 a.m. The overall study lasts for 6 months.

PREPARATION OF SAMPLES

The New Zealand white rabbits were sacrificed by decapitation, where the eyes were enucleated, and then opened by corneal section through the ora serrata. After removing the corneas, the iris was pulled out by a forceps where the eye lens and the vitreous humour (jelly structure) were jointly removed. The remaining eye cub, which contains the retina, was cut into two pieces and by the aid of a glass slide the retina was scrubbed and removed to previously sterilized and weighted dark brown glass vials. The glass vials were flushed by dry N_2 gas and kept at –20 °C for further analysis.

FTIR SPECTROSCOPY MEASUREMENTS

The weighted retinae were freeze-dried separately and mixed with KBr powder (2 mg retina: 98 mg KBr) then pressed to prepare the transparent KBr disks that will be used for the Fourier transformation infrared (FTIR) investigations.

FTIR measurements were carried out using Nicolet-iS5 infrared spectrometer (ThermoFisher Scientific Inc, Madison, USA) with effective resolution of 2 cm^{-1}. Each spectrum was derived from 100 sample interferograms. The spectrometer was operated under a continuous dry N_2 gas purge to remove interference from atmospheric CO_2 and H_2O vapor. The spectra were baseline corrected, then smoothed with Savitsky-Golay filter to remove the noise before Fourier

transformation. Three spectra from each sample were obtained and averaged using OriginPro9 software (Origin Lab Corporation, Northampton, MA, USA) to obtain the final average group spectrum which was normalized according to certain peaks and used in the figures.

STATISTICAL ANALYSIS

Data were expressed as the mean ± SD. Comparison between multiple groups was performed using analysis of variance (ANOVA); commercially available statistical software package (SPSS-11 for windows) was used where the significance level was set at $p < 0.05$.

RESULTS

The FTIR spectra of retinal tissues are quite complex and contain several bands arising from the contribution of different functional groups belonging to lipids, proteins, and others.

The FTIR spectra of retina for normal and treated animals covering the range 4000–900 cm^{-1} are recorded. Figure 1 shows that all vibrational frequency range corresponds to retinal tissue of normal group and rabbit's group is administered 5, 10 and 15 mg/kg tamoxifen daily for 2, 4 and 6 months respectively.

The detailed spectral analyses were performed in three distinct frequency ranges; 4000–3000 cm^{-1} (NH-OH region), 3000–2800 cm^{-1} (C–H stretching region) and 1700–900 cm^{-1} (Fingerprint region). The amide I band which appears at 1650 cm^{-1} will be considered separately since it consists of several underlying bands which correspond to different protein secondary structural components.

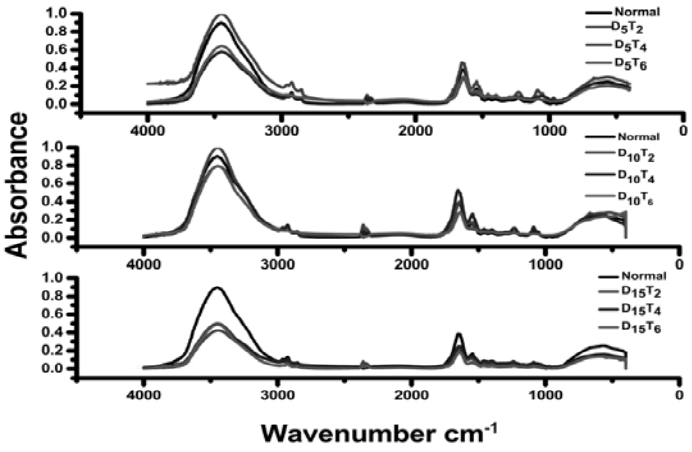

Fig. 1. Overlaid FTIR spectra for all studied groups.

NH-OH REGION

Figure 2 shows the NH-OH region of the retinal FTIR spectra (4000–3000 cm^{-1}) for normal and animals groups administered 5, 10 and 15 mg/kg of tamoxifen for 2, 4 and 6 months. The main band of the normal pattern was found at 3453±2 cm^{-1}. The curve enhancement procedure resolved this band into three structural components (Table 1) that were centered at 3595±1, 3453±2 and 3240±1 cm^{-1}, these bands correspond to (1) stretching O–H ($_{str}OH$), (2) stretching O–H asymmetric ($_{str}OH_{asym}$), and (3) stretching O–H symmetric ($_{str}OH_{sym}$) respectively as assignments previously mentioned by Dovbeshko *et al.* [7]. From Table 1, we observed the shifting of the $_{str}OH$ mode band to the lower wavenumbers with the significant increase ($p < 0.05$) of band width in $D_{10}T_2$, $D_{10}T_6$, $D_{15}T_2$ and $D_{15}T_4$ and splitting of the band after 4 and 6 months of administration of 5mg/kg tamoxifen. The $_{str}OH_{asym}$ band was also affected and split into two peaks in D_5T_2 and significant decrease ($p < 0.05$) in both wavenumber and band width in all groups except for $D_{15}T_6$. $_{str}OH_{sym}$ band had significant fluctuating changes ($p < 0.05$) in position and a significant increase in band width. The final observation is the appearance of a new band around 3092 cm^{-1} that related to (4) CH_{ring} after tamoxifen administration for all periods related to 5 mg/kg of tamoxifen.

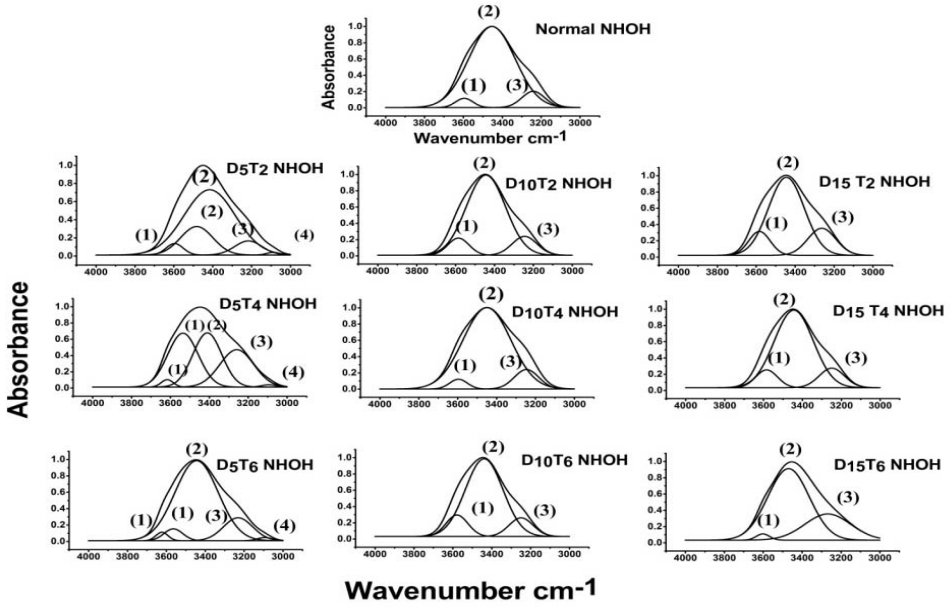

Fig. 2. NH-OH region of retina from normal animals group and groups administered 5, 10 and 15 mg/kg of tamoxifen for 2 , 4 and 6 months, showing the deconvoluted FTIR spectrum. (1) $_{str}OH$, (2) $_{str}OH_{asym}$, (4) $_{str}OH_{sym}$, and (6) CH_{ring}.

Table 1

Summary of the Fourier deconvolution and non linear curve fitting of the NH-OH region of retina from normal and different groups administered tamoxifen for 2, 4, 6 months

Groups	(1) $_{str}OH$		(2) $_{str}OH_{asym}$		(3) $_{str}OH_{sym}$	(4) CH_{ring}
Normal	3595±1 90±2		3453±2 238±3		3240±1 118±2	
D_5T_2	3596±2 88±1		3482±2 167±9	3416±11 263±12	†3228±5 †141±10	3089±3 67±9
D_5T_4	3616±1 63±2	3535±8 156±5	†3411±4 †148±10		†3258±8 †174±9	3094±2 76±7
D_5T_6	3623±2 62±3	3564±6 97±8	†3444±1 †221±1		†3231±1 †150±2	3094±2 77±3
$D_{10}T_2$	†3586±1 †109±2		†3444±1 †202±2		†3245±1 †128±1	
$D_{10}T_4$	3596±1 91±2		†3445±1 †245±1		3247±1 †126±1	
$D_{10}T_6$	†3579±1 †113±3		†3439±1 †193±4		3249±3 124±2	
$D_{15}T_2$	†3584±2 †110±4		†3445±1 †184±7		†3263±3 †144±2	
$D_{15}T_4$	†3584±1 †112±3		†3444±1 †200±3		†3249±1 †130±2	
$D_{15}T_6$	3601±3 †68±3		†3470±2 †213±2		†3268±6 †236±5	

First line in each cell indicates the vibrational frequency, while second line reflects the bandwidth
†Statistically significant.

CH REGION

Figure 3 indicated the absorption pattern of normal and retina's groups administered to 5, 10 and 15 mg/kg tamoxifen for 2, 4 and 6 months, respectively. The infrared absorption pattern of normal retina was characterized by three absorption bands in the IR range 3000–2800 cm^{-1}. The curve enhancement procedure that used to resolve any overlapping peaks confirms the presence of four bands that were centered at 2959±3 cm^{-1} with bandwidth of 17±1 cm^{-1}, 2925± 4 cm^{-1} with bandwidth of 25±1 cm^{-1}, 2870±6 with bandwidth of 33±2 and 2852± 3 cm^{-1} with corresponding bandwidth of 12±1 cm^{-1}. These bands can be assigned

as (1) CH_{3asym}, (2) CH_{2asym}, (3) CH_{3sym}, and (4) CH_{2sym} respectively as shown in Table 2. The assignment of the bands has been previously mentioned by Severcan *et al*. [27]. Among tamoxifen administration period, there were no significant changes in the number of estimated bands as well as in the wavenumber or the bandwidth (Table 2) except that CH_{3sym} after 6 months of 10 mg/kg tamoxifen ($D_{10}T_6$) had significant decrease ($p < 0.05$) in wavenumber, bandwidth and area. There were no significant changes in bandwidth or area to all groups compared to normal except for bandwidth and area of CH_{3sym} after 4 months of 5 mg/kg tamoxifen (D_5T_4), when a significant increase was observed.

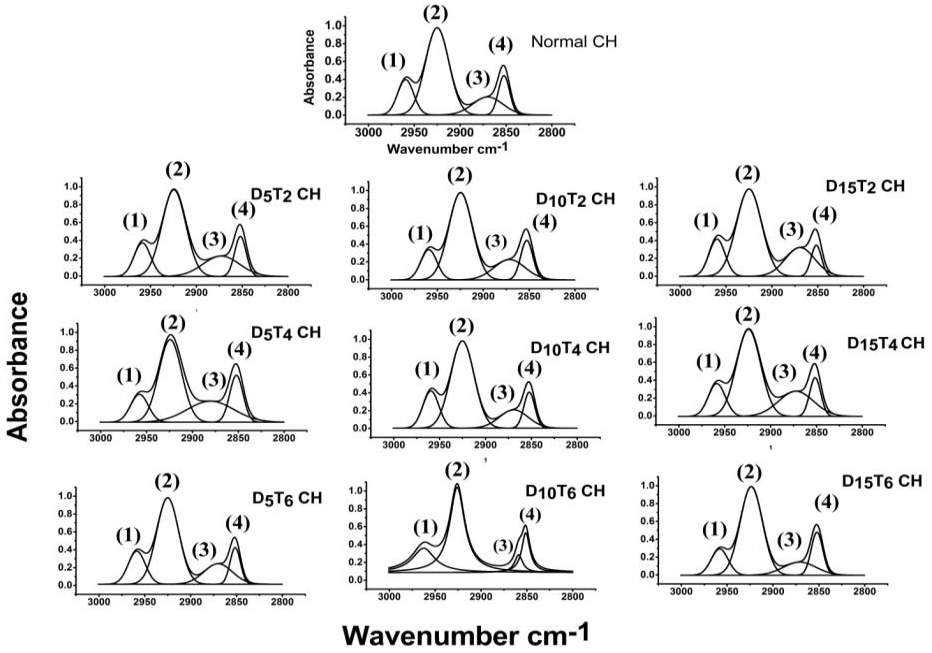

Fig. 3. CH region of retina from normal animals group and all groups administered to 5, 10 and 15 mg/kg of tamoxifen for 2, 4 and 6 months showing the deconvoluted FTIR spectrum. (1) $_{asym}CH_3$, (2) $_{asym}CH_2$, (3) $_{sym}CH_3$, and (4) $_{sym}CH_2$.

Table 2

Estimated structural components with their vibrational frequencies, bandwidth and area of the CH region of retina for normal and 10 mg/kg tamoxifen administered rabbits groups

Groups	**(1) CH_{3asym}**	**(2) CH_{2asym}**	**(3) CH_{3sym}**	**(4) CH_{2sym}**
Normal	2959±3 17±1 9±1	2925±4 25±1 31±2	2872±6 33±2 8±1	2852±2 12±1 7±0.5

Table 2

(continued)

Groups	(1) CH_{3asym}	(2) CH_{2asym}	(3) CH_{3sym}	(4) CH_{2sym}
D_5T_2	2959±4 18±1 9±1	2925±2 26±1 32±3	2873±3 40±5 11±1	2852±2 13±1 7±1
D_5T_4	2958±5 19±1 8±1	2924±3 25±3 29±2	2880±2 †51±2 †15±1	2852±2 15±2 10±1
D_5T_6	2959±3 19±1 9±1	2925±4 24±1 29±3	2870±2 31±1 9±2	2851±4 11±1 6±1
$D_{10}T_2$	2959±2 18±1 7±1	2924±2 26±1 31±1	2871±2 34±1 10±1	2852±3 13±1 7±1
$D_{10}T_4$	2959±2 17±1 9±0.4	2925±3 26±2 31±2	2869±3 31±2 8±1	2852±2 12±1 6±0.3
$D_{10}T_6$	2962±2 29±7 13±3	2926±2 20±1 29±1	†2861±1 †11±2 †3±1	2851±2 11±2 7±1
$D_{15}T_2$	2959±2 17±1 9±1	2924±4 27±2 34±3	2869±3 32±2 13±2	2851±4 11±2 5±0.3
$D_{15}T_4$	2958±4 19±1 9±1	2924±1 26±2 32±1	2872±1 38±1 14±1	2851±2 12±1 7±0.5
$D_{15}T_6$	2958±3 18±2 7±1	2923±3 24±3 30±2	2870±2 36±3 7±0.5	2852±3 13±1 8±0.4

First line in each cell indicates the vibrational frequency, while second line reflects the bandwidth and the third line indicates the area.

†Statistically significant.

FINGERPRINT REGION

The fingerprint region of the FTIR spectra covers the range 1700–900 cm^{-1}. In this range the absorption band between 1700 and 1600 cm^{-1} of the spectra which ascribed to C=O stretching vibrations, Amide I band, will be analyzed separately in details since it contains several underlying peaks which reflect the protein secondary structure characteristics. Figure 4 shows the FTIR absorption spectra in the range 1600 – 900 cm^{-1}. This figure indicates the presence of six bands in the normal pattern that was centered at (1) 1460±3 cm^{-1} ($_{bend}CH_2$), (2) 1398±2 cm^{-1}

($_{str}COO^{-}{}_{sym}$), (3) 1301±3 cm^{-1} ($_{def}CH_3$ deformation), (4) 1226±2 cm^{-1} ($_{str}PO2^{-}{}_{asym}$), (5) 1177±2 cm^{-1} ($_{str}COOC_{asym}$), (6) 1089±3 cm^{-1} ($_{str}PO2^{-}{}_{sym}$), and (7) 1050±1 cm^{-1} ($_{str}COC$) as given in Table 3. The bands assignments have been indicated by Jung [18] and Stuart [29].

Also Figure 4 showed the spectra of tamoxifen administered groups (5, 10 and 15 mg/kg) for 2, 4 and 6 months. As a result of tamoxifen administration, six observations can be concluded from Table 3: (1) Increase the number of bands estimated after 6 months of 5, 10, and 15 mg/kg tamoxifen to 11, 12 and 13 bands, respectively. (2) Splitting of bending CH_2 after any dose of tamoxifen except $D_{10}T_4$ and splitting of $_{str}COO^{-}{}_{sym}$ in $D_{10}T_6$, $D_{15}T_6$. (3) Splitting of $_{def}CH_3$ for all groups except $D_{10}T_4$. (4) Significant increase ($p < 0.05$) of $_{str}PO_2^{-}{}_{asym}$ after 6 months of any dose of tamoxifen. (5) Significant decrease ($p < 0.05$) of band position of $_{str}COOC_{asym}$ for all groups compared to normal. (6) Splitting of $_{str}COC$ in D_5T_6 and disappearance of this mode of action after 10 and 15 mg/kg of tamoxifen.

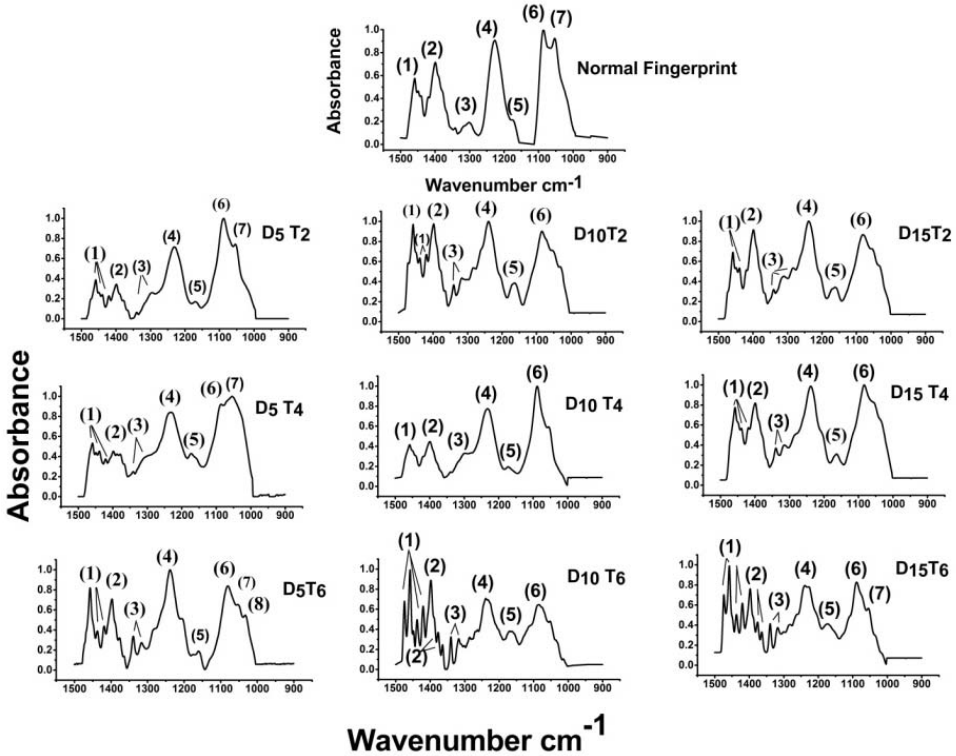

Fig. 4. FTIR spectra of the fingerprint region of normal group and all groups administered to 5, 10 and 15 mg/kg of tamoxifen for 2, 4 and 6 months. The numbers above the peaks are to facilitate their assignment.

Table 3

Vibrational frequencies of the estimated bands in fingerprint region of normal and different groups administered tamoxifen

Group	(1) $_{bend}CH_2$	(2) $_{str}COO^-_{sym}$	(3) $_{def}CH_3$	(4) $_{str}PO_2^-_{asym}$	(5) $_{str}COOC_{asym}$	(6) $_{str}PO_2^-_{sym}$	(7) $_{str}COC$
Normal	1460±3	1398±2	1301 ±3	1226±4	1177±2	1089±1	1050±1
D_5T_2	1463±3 1440±1 1420±1	1402±2	1339±1 1300±2	1231±3	†1168±1	1090±2	1055±3
D_5T_4	1460±1 1440±1 1420±2	1402±2	1343±2 1311±3	1229±3	†1163±3	1085±3	1054±3
D_5T_6	1457±3 1437±1 1422±1	1396±4	1339±2 1318±1	†1237±1	†1159±2	1080±5	1030±2 1055±2
$D_{10}T_2$	1458±2 1440±1 1420±1	1398±3	1341±1 1317±2	1231±2	†1166±2	1084±4	
$D_{10}T_4$	1458±3	1401±2	1308±1	1232±1	†1147±1	1088±2	
$D_{10}T_6$	1476±3 1458±2 1437±3 1421±2	1398±3 1375±2 1364±1	1341±1 1319±1	†1238±3	†1166±1	1086±3	
$D_{15}T_2$	1459±2 1438±1	1398±1	1341±1 1311±3 1285±1	1233±3	†1160±1	1085±4	
$D_{15}T_4$	1459±3 1440±1 1420±2	1399±1	1338±2 1315±1	1234±4	†1164±1	1086±4	
$D_{15}T_6$	1474±1 1459±2 1439±1 1420±3	1398±1 1376±1 1364±3	1342±1 1318±1	†1239±2	†1160±1	1090±3	1053±3

†Statistically significant

AMIDE I BAND

Analysis of the amide I band (Fig. 5) showed the curve enhancement procedure for normal group and animals treated with 5, 10 and 15 mg/kg of tamoxifen for 2, 4 and 6 months. The analysis resolved the contour of the normal band into 4 compositional bands that were centered at 1674±2 cm^{-1} (β-Turns, labeled as 1), 1653±1 cm^{-1} (α-helix, labeled as 2) and 1636±1 and 1624±1 cm^{-1}

(β-Sheet, labeled as 3). Table 4 indicates that the distribution of normal protein secondary structure components – that were calculated as the area percentage – were 11.49±0.5% for β-Turns, 59.1±3% for α-helix and 29.41±2% for β-Sheet. The assignment of the bands was indicated by Severcan and Haris [26] and Fuller *et al*. [10].

After 5 mg/kg tamoxifen administration for all periods, the contour of amide I band was resolved into 7 structural components. For D_{10} T_2, $D_{15}T_4$ and $D_{15}T_6$ amide I resolved into 5 structural components. There was detected β-sheet in all groups with frequency > 1620 cm^{-1} assigned as intermolecular β-sheets.

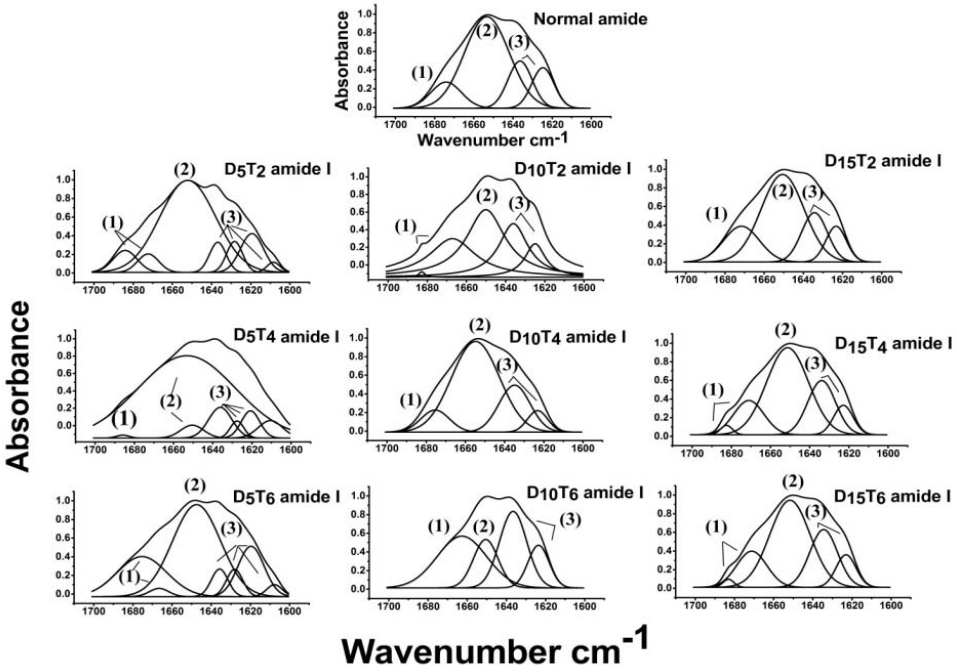

Fig. 5. Amid I region (1700:1600 cm^{-1}) of deconvoluted FTIR spectrum for retina for normal and treated animals with 5, 10 and 15 mg/kg of tamoxifen for 2, 4 and 6 months. (1) β-turns, (2) α-helix, and (3) β-sheet.

Table 4 shows that the relative distribution of the structural component was differrent. The α-helix content was significantly decreased ($p < 0.05$) for D_5T_6, $D_{10}T_2$, $D_{10}T_6$ and all periods of 15 mg/kg of tamoxifen, concomitant with an increase in β-Turns structures. For D_5T_4 the increased of α-helix is associated with a reduced β-Turns. The β-Sheet structure shows a significant decrease in D_5T_4 and a significant increase for $D_{10}T_6$.

Table 4

Retinal protein secondary structure components after different doses of tamoxifen administration, expressed as area percentage of each structural component relative to the total band area

Groups	β-turns%	α-helix%	β-sheet%
Normal	11.49±0.5	59.10±2	29.41±2
D_5T_2	11.39±3.5	63.48±4	25.13±2
D_5T_4	†0.38±0.4	†81.30±5	†18.32±1
D_5T_6	†23.90±1	†49.19±2	26.91±1
$D_{10}T_2$	†27.21±2	†39.14±2	33.65±2.4
$D_{10}T_4$	9.20±2	63.15±5	27.65±1
$D_{10}T_6$	†38.03±4	†17.65±2	†44.32±4
$D_{15}T_2$	†18.13±0.5	†53.43±1	28.44±2
$D_{15}T_4$	†16.67±1	†53.12±1	30.21±3
$D_{15}T_6$	†17.01±1	†50.56±1	32.43±1

† Statistically significant

DISCUSSION

Fourier transform infrared (FTIR) spectroscopy and imaging is an emerging technique in the field of *ex vivo* diagnostics. The infrared spectra of single cells and intact tissues originating from dozens of species and cell types have been analyzed by several groups worldwide [4, 12, 19, 32]. These studies have not only provided important information regarding the macromolecular contents and their distribution in a cell or tissue sample but they have also demonstrated the ability of FTIR spectroscopy to differentiate between diseased and non-diseased states [24],

determine cell cycle stage [31] and monitor cell death [16]. By measuring the absorption of infrared light by a sample, the characteristic energies and intensities of absorbance bands of cellular macromolecules can be detected and assigned, including carbohydrates, lipids, proteoglycans, collagens, nucleic acids and proteins [33]. Moreover, details about the structure and local environment of these macromolecules can also be elucidated.

In the present study, tamoxifen did not affect the CH stretching modes of rabbit retina, but the NH-OH region of the rabbit retina has been affected by the tamoxifen administration where there is a different interaction/binding mechanism and production of various states in the system, as well as different configurations and conformations co-exist in the system after tamoxifen administration especially in the OH modes. Also some hydrogen bonds have been destructed or weaker hydrogen bonds have existed. The splitting of the band reflects different interaction binding mechanisms and the variation of the surrounding environment. The wavenumber of the CH_3 symmetric stretching band shifts to lower values in $D_{10}T_6$, indicating an increase of the lipid chains [27]. In addition, the marked change in wavenumber of the fingerprint region of retina's groups administered to tamoxifen attributed to oxidative stress induced by tamoxifen (Table 3). Oxidative changes have been reported that indomethacin, tamoxifen, thioridazine, and chloroquine all produce retinopathies via a common mechanism – they produce ocular oxidative stress [5, 30]. The $_{bend}CH_2$ band detected at 1460±3 cm^{-1} due to the scissoring motion of the lipid molecule was affected by splitting in the larger period of tamoxifen administration indicating a disturbance in the lipid order. The change in band position of $_{str}PO_{2asym}$ band reflects different interaction mechanisms that appear after 6 months of tamoxifen administration. This may involve phosphor-lipids, genetic material or phosphate sugar that represent the structural constituents of the retinal tissue.

Tamoxifen is a nonsteroidal antiestrogen, which belongs to the family of selective ER modulators, drugs that have the ability to occupy ERs (ERα and ERβ), acting as ER antagonists in the breast tissue. ERα and ERβ are also present within the neural retina and the pigment epithelium of men and women, where tamoxifen is reported to decrease glutamate uptake [8]. Tamoxifen retinopathy is typically characterized by the presence of small refractile deposits in the nerve fiber and inner plexiform layers, primarily in the perifoveal area [13]. Due to tamoxifen's amphiphilic nature, it is suggested that it binds to polar lipids, accumulates in lysosomes, and causes cell oxidative damage. Numerous researchers have suggested that tamoxifen retinopathy is not caused by actions of tamoxifen on ERs, but stems instead from tamoxifen's cationic amphiphilic properties [6, 17–28].

The amide I absorption band arises mainly from C=O the stretching vibration with minor contributions from the out-of-phase CN stretching vibration, the CCN deformation and the NH in-plane band. The Amide I band is suggesting a conformational change in α-helixes [1]. Table 4 indicated that amide I band

suggests that proteins lose their structure due to a significant decrease observed as induced from free radical reactions. The exposure of proteins to free radicals induces secondary structural changes, since secondary structure is stabilized by hydrogen bonding of peptide backbone. Proteins are organized into α-helixes, but the hydrogen bond is damaged, so the chains open and are more prone to free radicals, leading to the change of α-helix. The change of dipole moment of peptide bond, as it is shown in equation (1) at resonance structures, leads to a change in the orientation of amino groups (NH) to the carbonyl group C=O, resulting in the destruction of α-helix and the secondary structure of proteins.

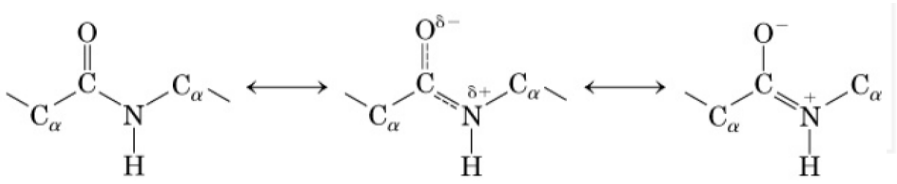

(1)

During the administration interval of tamoxifen β-turn structure was increased. β-turns are the smallest type of protein secondary structure, joining other elements of secondary structure such as α-helix and β-sheets and abruptly change the direction of the polypeptide chain and may dictate the folding of longer polypeptide chains. β-turns are common conformations that enable protein to adopt globular structures, and may serve as a nucleation site for folding/refolding of proteins [11]. Their formation is often rate limiting for folding where protein stability is intimately connected with protein folding. Also, the detected β-sheets with frequency > 1620 are assigned as intramolecular β-sheets. These sheets are associated with protein folding. Accordingly, retinal proteins are more folded during tamoxifen administration.

CONCLUSIONS

FTIR spectroscopy is an excellent technique for the investigation of biological structures due to its sensitivity and ability to give valuable information about the functional groups, which might have diagnostic value for biological systems. These data suggest a molecular mechanism by which tamoxifen can cause retinal secondary structure changes and have implications for the clinical use of tamoxifen and related antiestrogens suggesting that people using tamoxifen should receive an eye exam at least as often as recommended for middle-aged people.

Acknowledgements. We thank Dr. Sherif S. Mahmoud for expert technical assistance with the FTIR measurements and his cooperation.

REFERENCES

1. ANASTASSOPOULOU, J., E. BOUKAKI, C. CONTI, P. FERRARIS, E. GIORGINI, C. RUBINI, *et al*., Microimaging FT-IR spectroscopy on pathological breast tissues, *Vibrational Spectroscopy*, 2009, **51**, 270–275.
2. ASHFORD, A.R. *et al*., Reversible ocular toxicity related to tamoxifen therapy, *Cancer*, 1988, **61**, 33–35.
3. AZIZI-MALEKABADI, H., M. POURGANJI, H. ZABIHI, M. SAEEDJALALI, M. HOSSEINI, Tamoxifen antagonizes the effects of ovarian hormones to induce anxiety and depression-like behavior in rats, *Arq. Neuropsiquiatr.*, 2015, **73**(2), 132–139.
4. CARTER, E.A., K.K. TAM, R.S. ARMSTRONG, P.A. LAY, Vibrational spectroscopic mapping and imaging of tissues and cells, *Biophys. Rev*., 2009, **1**, 95–103.
5. CHO, K.S., Y.H. YOON, J.A. CHOI, S.J. LEE, J.Y. KOH, Induction of autophagy and cell death by tamoxifen in cultured retinal pigment epithelial and photoreceptor cells, *Invest. Ophthalmol. Vis. Sci.*, 2012, 9, **53**(9), 5344–5353.
6. CHUNG, H., D. KIM, S.H. AHN, J.G. KIM, J.Y. LEE, J.Y. LIM, *et al.*, Early detection of tamoxifen-induced maculopathy in patients with low cumulative doses of tamoxifen, *Ophthalmic Surg. Lasers Imaging*, 2010, **41**, el–e5
7. DOVBESHKO, G.I., N.Y. GRIDINA, E.B. KRUGLOVA, O.P. PASHCHUK, FTIR spectroscopy studies of nucleic acid damage, *Talanta*, 2000, **53**, 233–246.
8. EISNER, A., S.W. LUOH, Breast cancer medications and vision: effects of treatments for early-stage disease, *Curr. Eye Res.*, 2011, **36**(10), 867–885.
9. EISNER, A., E.J. THIELMAN, J. FALARDEAU, J.T. VETTO, Vitreo-retinal traction and anastrozole use, *Breast Cancer Res. Treat*., 2009, **117**(1), 9–16.
10. FULLER, A.A., D. DU, F. LIU, J. DAVOREN, G. BHABHA, G. KROON, *et al*., Evaluating-turn mimics as sheet fold nucleators, *PNAS*, 2009, **106**, 11067–11072.
11. GAMAL, E.M., E.M. ALY, S.S MAHMOUD, M.S. TALAAT, A.S. SALLAM, FTIR assessment of the effect of *Ginkgo biloba* leave extract (EGb 761) on mammalian retina, *Cell Biochem. Biophys.*, 2011, **61**(1), 169–177.
12. GAZI, E, P. GARDNER, Preparation of tissues and cells for infrared and Raman spectroscopy and imaging, In: G. Srinivasan, ed., *Vibrational Spectroscopic Imaging for Biomedical Applications*, New York, McGraw-Hill, 2010, pp. 59–98.
13. GEORGALAS, I., T. PARASKEVOPOULOS, D. PAPACONSTANINOU, D. BROUZAS, C. KOUTSANDREA, Large bilateral foveal cysts in the inner retina of a patient treated with tamoxifen, diagnosed with Fourier-domain optical coherence tomography, *Clin. Ophthalmol*., 2013, **7**, 707–709.
14. GORIN, M. B. *et al*., Long-term tamoxifen citrate use and potential ocular toxicity, *Am. J. Ophthalmol.*, 1998, **125**, 493–501.
15. GREAVES, P., R. GOONETILLEKE, G. NUNN, J. TOPHAM, T. ORTON, Two-year carcinogenicity study of tamoxifen in Alderley Park Wistar-derived rats, *Cancer Res.*, 1993, **53**(17), 3919–3924.
16. GU, L., L. XIE, W. YAO, W. KA, D. SUN, *et al*., FTIR spectroscopy studies on the apoptosis-promoting effect of TFAR19 on the erythroleukemia cell line MEL, *Journal of Biomedical Engineering*, 2004, **21**, 449–452.
17. HAGER, T., S. HOFFMANN, B. SEITZ, Unusual symptoms for tamoxifen-associated maculopathy, *Ophthalmologie*, 2010, **107**(8), 750–752.
18. JUNG, C. Review insight into protein structure and protein-ligand recognition by Fourier transform infrared spectroscopy, *Journal of Molecular Recognition*, 2000, **13**, 325–351.
19. MALEK, K., B.R. WOOD, K.R. BAMBERY, *FTIR Imaging of Tissues: Techniques and Methods of Analysis*, In: M. Baranska, ed., *Optical Spectroscopy and Computational Methods in Biology and Medicine*, Springer Science, 2014, pp. 419–474.

20. MORAD, S.A., J.C. LEVIN, S.S. SHANMUGAVELANDY, M. KESTER, G. FABRIAS, C. BEDIA, *et al.,* Ceramide--antiestrogen nanoliposomal combinations-novel impact of hormonal therapy in hormone-insensitive breast cancer, *Mol. Cancer Ther.*, 2012, **11**(11), 2352–2361.
21. OMOTI, A.E., C.E. OMOTI, Ocular toxicity of systemic anticancer chemotherapy, *Pharm. Pract.* (Granada), 2006 **4**(2), 55–59.
22. PAVLIDIS, N. A. *et al*., Clear evidence that long-term, low-dose tamoxifen treatment can induce ocular toxicity. A prospective study of 63 patients, *Cancer*, 1992, **69**, 2961–2964.
23. RAMBAU, P., N. MASALU, K. JACKSON, P. CHALYA, P. SERRA, S. BRAVACCINI, Triple negative breast cancer in a poor resource setting in North-Western Tanzania: a preliminary study of 52 patients, *BMC Res. Notes*, 2014, **26**, 7:399.
24. RUBIN, S., F. BONNIER, C. SANDT, L. VENTEO, M. PLUOT, *et al.*, Analysis of structural changes in normal and aneurismal human aortic tissues using FTIR microscopy, *Biopolymers*, 2008, **89**, 160–169.
25. SALOMAO, S.R., S.E. WATANABE, A. BEREZOVSKY, M. MOTONO, Multifocal electroretinography, color discrimination and ocular toxicity in tamoxifen use, *Curr. Eye Res.*, 2007, **32**, 345–352.
26. SEVERCAN, F., P.I HARIS, Fourier transform infrared spectroscopy suggests unfolding of loop structures precedes complete unfolding of pig citrate synthase, *Biopolymers,* 2003, **57**, 160–168.
27. SEVERCAN, F., N. TOYRAN, N. KAPTAN, B. TURAN, Fourier transform infrared study of the effect of diabetes on rat liver and heart tissues in the C–H region, *Talanta*, 2000, **53**(1) 55–59.
28. SRIKANTIA, N., S. MUKESH, M. KRISHNASWAMY, Crystalline maculopathy: a rare complication of tamoxifen therapy, *J. Cancer Res. Ther*., 2010, **6**(3), 313–315.
29. STUART, B. *Biological application of infrared spectroscopy*. ACOL Series, Wiley, Chichester, UK, 1997, P139.
30. TOLER, S.M. Oxidative stress plays an important role in the pathogenesis of drug-induced retinopathy, *Exp. Biol. Med.* (Maywood), 2004, **229**(7), 607–615.
31. WHELAN, D.R., K.R. BAMBERY, L. PUSKAR, D. MCNAUGHTON, B.R. WOOD, Synchrotron Fourier transform infrared (FTIR) analysis of single living cells progressing through the cell cycle, *The Analyst*, 2013, **138**, 3891–3899.
32. WOOD, B.R., T. CHERNENKO, C. MATTHAUS, M. DIEM, C. CHONG, *et al*., Shedding new light on the molecular architecture of oocytes using a combination of synchrotron Fourier transform-infrared and Raman spectroscopic mapping, *Anal. Chem.*, 2008, **80**, 9065–9072.
33. ZOHDI, V., D.R. WHELAN, B.R. WOOD, J.T. PEARSON, K.R. BAMBERY, M.J. BLACK, Importance of tissue preparation methods in FTIR micro-spectroscopical analysis of biological tissues: traps for new users, *PLoS One*, 2015, 24, **10**(2).